

High-Power Fiber Lasers for Directed-Energy Applications

P. Sprangle,¹ A. Ting,¹ J. Peñano,¹ R. Fischer,¹ and B. Hafizi²

¹*Plasma Physics Division*

²*Icarus Research, Inc.*

High-power fiber lasers can be incoherently combined to form the basis of a high-energy laser system for directed-energy applications. These applications include tactical directed energy and power beaming. Incoherent combining of fiber lasers has a number of advantages over other laser beam combining methods. The incoherently combined laser system is relatively simple, highly efficient, compact, robust, low-maintenance, and reliable. In this article, we characterize the atmospheric propagation of incoherently combined, high optical quality laser beams and compare them with other types of laser beams and combining methods. For tactical directed-energy applications, we find that the propagation efficiency of incoherently combined high optical quality beams is near the theoretical upper limit for any laser system with the same beam director and total power. We present results of the first atmospheric propagation experiments using incoherently combined, kilowatt-class, single-mode fiber lasers. These NRL field experiments combined four fiber lasers using a beam director consisting of individually controlled steering mirrors. The transmitted continuous-wave power was 3 kW at a range of 1.2 km with a demonstrated propagation efficiency of ~90% in moderate atmospheric turbulence. The experimental results are found to be in good agreement with simulations and theory.

INTRODUCTION

The successful development of laser weapons promises to have a profound impact on military missions throughout the services. A directed-energy (DE) laser system must be capable of delivering hundreds of kilowatts of average power to a target at multi-kilometer ranges through adverse atmospheric conditions. In addition, the laser system must be efficient, compact, robust, and reliable. While a great deal of progress has been made toward this objective, the goal will soon receive a significant boost due to advances in high-power fiber laser technology. High-power fiber lasers can also have applications in the area of power beaming, e.g., to UAVs and low-orbit satellites.

To achieve the total laser power needed for tactical DE and power beaming applications it is necessary to combine a large number of fiber lasers. Lasers can be combined coherently, spectrally, or incoherently. This article focuses on incoherent combining of high-power, high optical quality fiber lasers. This laser beam combining approach has a number of advantages over coherent or spectral combining.

In this article we discuss the characteristics of high-power fiber lasers and the progress made in increasing the output power of these devices while maintaining high optical quality. In addition, we discuss and compare the propagation efficiency of incoherently combined fiber laser arrays and coherently combined arrays in realistic atmospheric conditions for multi-kilometer propagation ranges. We conclude by present-

ing results from the first field propagation experiments which demonstrate high-power, kilometer-range incoherent combining. In these NRL experiments, four single-mode fiber lasers capable of transmitting a combined continuous-wave (CW) power of 6.2 kW were incoherently combined on a target at a range of 1.2 km. The total volume occupied by the four fiber lasers, including power supply, diode pump lasers, and fibers, is less than 2 m³. In the experiments, a total of 3 kW was transmitted over a 1.2 km range to a 10 cm radius target with the lasers at half power. Propagation efficiencies of ~90% were demonstrated in a moderately turbulent environment.

HIGH-POWER FIBER LASERS

Although a number of companies manufacture high-power fiber lasers, IPG Photonics Corp. (MA) currently has the most powerful, with over 3 kW per fiber of single-mode optical radiation.¹ Nufern (CT) now has a 1 kW, single-mode fiber laser available.² The term “single-mode” laser beam is synonymous with a diffraction-limited ideal Gaussian beam. The optical quality of a laser beam is measured in terms of the parameter M^2 , which characterizes the laser beam spreading angle. An ideal Gaussian beam, i.e., single-mode beam, is characterized by an M^2 of unity and has the smallest spreading angle of any beam profile with the same spot size (radius). Multi-mode beams have an M^2 greater than unity. The diffraction (spreading) angle of multi-mode beams is M^2 times greater than

Report Documentation Page				Form Approved OMB No. 0704-0188	
Public reporting burden for the collection of information is estimated to average 1 hour per response, including the time for reviewing instructions, searching existing data sources, gathering and maintaining the data needed, and completing and reviewing the collection of information. Send comments regarding this burden estimate or any other aspect of this collection of information, including suggestions for reducing this burden, to Washington Headquarters Services, Directorate for Information Operations and Reports, 1215 Jefferson Davis Highway, Suite 1204, Arlington VA 22202-4302. Respondents should be aware that notwithstanding any other provision of law, no person shall be subject to a penalty for failing to comply with a collection of information if it does not display a currently valid OMB control number.					
1. REPORT DATE 2008		2. REPORT TYPE		3. DATES COVERED 00-00-2008 to 00-00-2008	
4. TITLE AND SUBTITLE High-Power Fiber Lasers for Directed-Energy Applications				5a. CONTRACT NUMBER	
				5b. GRANT NUMBER	
				5c. PROGRAM ELEMENT NUMBER	
6. AUTHOR(S)				5d. PROJECT NUMBER	
				5e. TASK NUMBER	
				5f. WORK UNIT NUMBER	
7. PERFORMING ORGANIZATION NAME(S) AND ADDRESS(ES) Naval Research Laboratory, 4555 Overlook Avenue SW, Washington, DC, 20375				8. PERFORMING ORGANIZATION REPORT NUMBER	
9. SPONSORING/MONITORING AGENCY NAME(S) AND ADDRESS(ES)				10. SPONSOR/MONITOR'S ACRONYM(S)	
				11. SPONSOR/MONITOR'S REPORT NUMBER(S)	
12. DISTRIBUTION/AVAILABILITY STATEMENT Approved for public release; distribution unlimited					
13. SUPPLEMENTARY NOTES					
14. ABSTRACT					
15. SUBJECT TERMS					
16. SECURITY CLASSIFICATION OF:			17. LIMITATION OF ABSTRACT Same as Report (SAR)	18. NUMBER OF PAGES 11	19a. NAME OF RESPONSIBLE PERSON
a. REPORT unclassified	b. ABSTRACT unclassified	c. THIS PAGE unclassified			

that of a single-mode (ideal Gaussian) beam. For long-range propagation, single-mode beams are necessary.

Figure 1 illustrates the progress made in recent years in increasing the power in single-mode fiber lasers. It is anticipated that the power output of single-mode fiber lasers will reach a plateau of ~ 5 kW/fiber in approximately one year. Multi-kilowatt, single-mode fiber lasers are robust, compact, and have high wall-plug efficiency, random polarization, and large bandwidth ($\sim 0.1\%$). A 1 kW, single-mode IPG fiber laser module, operating at wavelength $\lambda = 1.075$ μm , excluding power supply, measures $w \times h \times d \sim 60 \text{ cm} \times 33 \text{ cm} \times 5 \text{ cm}$, weighs approximately 20 lbs, has a wall-plug efficiency of $>30\%$, and has an operating lifetime in excess of 10,000 hrs. Figure 2 shows a 1.2 kW fiber laser module manufactured by IPG. The total weight of a 2 kW IPG fiber laser, including power supply, is ~ 330 lbs. Because of the high operating efficiency, only a moderate degree of water cooling is required, i.e., ~ 2 gallons/minute/kW. To operate in a single mode, the optical core radius of the fiber must be sufficiently small. For example, the IPG single-mode 1 kW fiber lasers have an optical core radius of ~ 15 μm . Multi-mode IPG fibers, on the other hand, operating at 10 kW (20 kW) per fiber have an optical core radius of ~ 100 μm (~ 200 μm) and $M^2 \sim 13$ ($M^2 \sim 38$). These higher-power fiber lasers with larger values of M^2 have a more limited propagation range.

FIBER LASER COMBINING

To achieve the power levels needed for DE applications it is necessary to combine a large number of fiber lasers either coherently, spectrally, or incoherently. Coherent and spectral combining of laser beams can, in principle, result in a smaller size beam director. Coherent combining seeks to construct a phase-locked optical wavefront from many individual lasers, thus increasing the effective laser spot size and extending the propagation range. However, this approach requires extremely narrow laser linewidths and precise control

of the polarization and phase of the individual lasers. Fiber lasers with the narrow line widths required for coherent combining are currently limited in power to less than a few hundred watts per fiber due to inherent nonlinearities which broaden the linewidth. Spectral combining uses gratings to combine a large number of beams with slightly different wavelengths. This approach is also limited by the fiber laser bandwidth and the requirement that the lasers have a well-defined polarization. To date, the highest total power achieved through coherent or spectral combining is less than 1 kW. Using currently available fiber lasers, a coherently or spectrally combined DE system would be complex and require an extremely large number of lasers.

Incoherent combining has a number of advantages over coherent and spectral combining. This approach does not require narrow linewidths or phase/polarization locking of the individual lasers. Hence, it allows for the use of higher-power, multi-kilowatt fiber lasers and is much easier to implement. Incoherent combining of laser beams is achieved by overlapping the individual laser beams on a target with a beam director consisting of independently controlled steering mirrors and beam expanders³ as shown in Fig. 3. To limit diffractive spreading over the propagation range, the spot size of the beams must be large enough at the source and the beams must have good optical quality. In the absence of turbulence, the effective range of an incoherently combined array of single-mode lasers is determined by the Rayleigh range (Z_R) of an individual beam, which is given by $Z_R = \pi R_o^2 / \lambda$, where R_o is the initial beam spot size and λ is the laser wavelength. To achieve efficient propagation, the distance to the target (target range), L , should be less than $\sim 2Z_R$. For example, a single-mode fiber laser with initial spot size $R_o = 4$ cm and wavelength $\lambda = 1$ μm has a Rayleigh range of ~ 5 km, so the target range should be less than ~ 10 km to avoid significant diffractive spreading. Usually, however, the spreading of the beam is dominated by atmospheric turbulence and not diffraction. This situation is discussed in the next section.

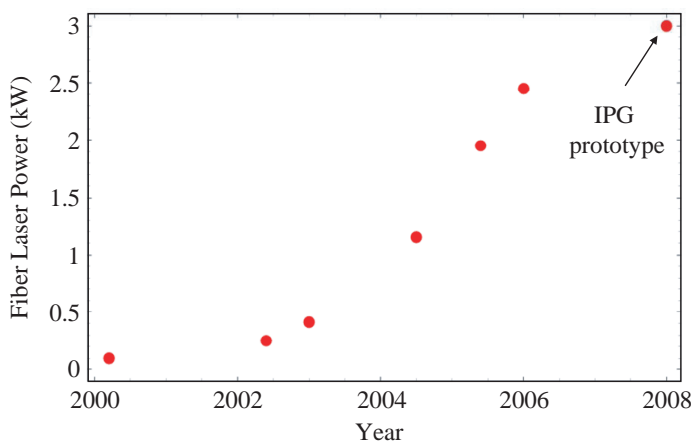
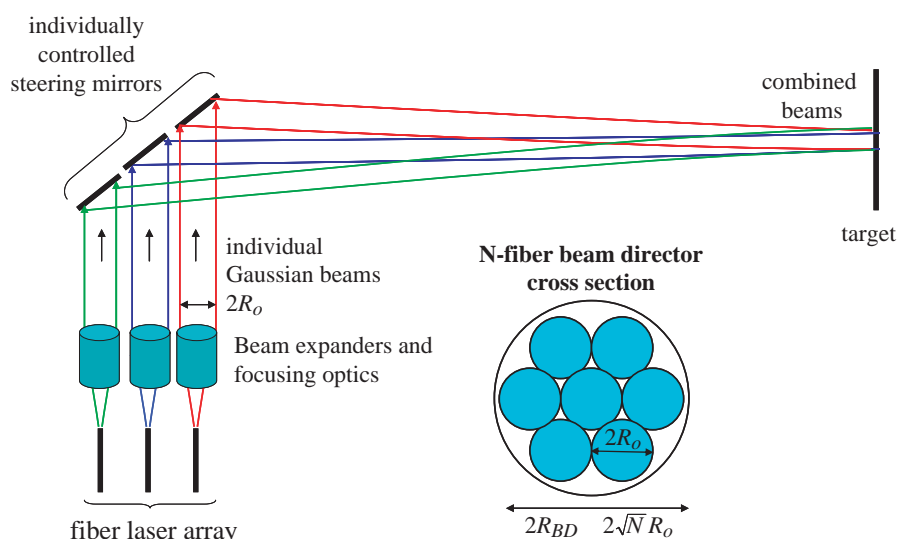
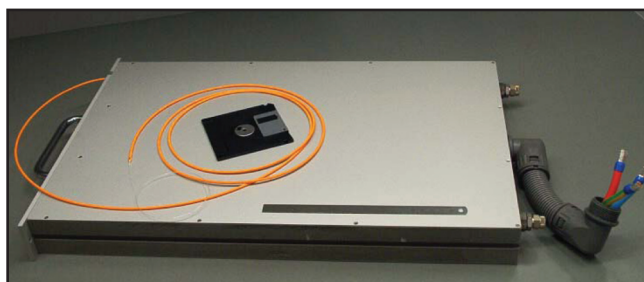


FIGURE 1
Progress made in increasing the power per fiber in single-mode fiber lasers.

FIGURE 2

IPG Photonics 1.2 kW fiber laser module. Module has dimensions $60 \times 33 \times 5$ cm, weight ~ 20 lbs, and wall-plug efficiency $\sim 30\%$.

**FIGURE 3**

Schematic diagram of incoherently combined fiber laser beams directed to a target.

Because incoherent combining allows for a higher power per fiber, the laser system is compact and readily scalable to power levels needed for DE applications. For N incoherently combined fiber lasers, the total transmitted power is N times the power in the individual fiber, and the beam director radius is $R_{BD} \approx \sqrt{N}R_o$. A 500 kW laser system would consist of 100 fiber lasers (5 kW/fiber), have a beam director radius of ~ 40 cm, and, excluding power supply, the fibers and pump diodes would occupy a volume of ~ 8 m³.

ATMOSPHERIC PROPAGATION OF LASER BEAMS

The physical processes affecting the propagation of high-power laser beams in the atmosphere are complex and interrelated. These processes include diffraction, molecular/aerosol scattering and absorption, turbulence produced by air density fluctuations, thermal blooming, and others. While it is beyond the scope of this article to consider these physical processes in detail, for the purpose of estimating and comparing the propagation efficiency of combined single-mode and multi-mode fiber lasers we consider some of the more important processes in a simplified manner. We also

discuss the use of tip-tilt compensation in the beam director to correct for the wander of the laser beam centroid due to turbulence, and quantify its limitations.

The minimum laser beam spot size, or radius, is obtained by adjusting the focal length of the transmitted beam so it equals the distance to the target, or range L . The laser beam spot size on target is then given by $R = \Theta_{\text{spread}} L$ where the spreading angle Θ_{spread} is the sum of contributions from diffraction, Θ_{diff} , atmospheric turbulence, Θ_{turb} , mechanical jitter, Θ_{jitter} , and thermal blooming, Θ_{bloom} . Thermal blooming, i.e., the self-defocusing of the laser due to absorption and the subsequent heating of the air, can be partially mitigated by propagating in an atmospheric transmission window where the absorption is low. Fortunately the fiber laser wavelength, $\lambda = 1.075$ μm , is near a narrow water vapor transmission window centered at $\lambda = 1.045$ μm . In the presence of water-based aerosols the actual transmission window is broadened⁴ and easily includes the fiber laser wavelength. For total laser power levels less than ~ 100 kW, and depending on the transverse air flow and atmospheric absorption, thermal blooming effects can usually be neglected.³ Thermal blooming near the beam director can be eliminated by introduc-

ing a transverse air flow.⁵ For the purposes of this discussion we will also neglect the small mechanical jitter contribution and concentrate on the dominant effects of turbulence and diffraction.

Atmospheric turbulence strength is described by the parameter C_n^2 , which characterizes the amplitude of density fluctuations in the air. C_n^2 normally ranges from $10^{-15} \text{ m}^{-2/3}$ (weak turbulence) to $10^{-13} \text{ m}^{-2/3}$ (very strong turbulence). The effect of turbulence on laser beam propagation is characterized by the Fried parameter (transverse coherence length), r_o , which is a function of C_n^2 and propagation range. The Fried parameter varies from tens of centimeters for weak turbulence conditions to fractions of a centimeter for strong turbulence. The spreading angle of a laser beam due to atmospheric turbulence is $\Theta_{\text{turb}} = 1.6 \lambda / \pi r_o$.^{6,7}

Comparison of Single- and Multi-Mode Propagation

The diffractive spreading angle of an individual laser beam is $\Theta_{\text{diff}} = M^2 \lambda / (\pi R_o)$. The goal of coherent combining is to reduce the diffractive spreading angle by phase locking and polarization locking N individual single-mode lasers, thus increasing the effective spot size by a factor of \sqrt{N} . For single-mode fiber lasers propagating over long distances, turbulence spreading dominates diffractive spreading, i.e., $\Theta_{\text{turb}} \gg \Theta_{\text{diff}}$, since the Fried parameter is usually less than the initial laser spot size, $r_o \ll R_o$. On the other hand, for highly multi-mode fibers ($M^2 \gg 1$), the diffractive spreading angle can be large, i.e., $\Theta_{\text{diff}} > \Theta_{\text{turb}}$. These differences between single-mode and multi-mode fibers have important consequences for their propagation efficiency and the use of adaptive optics to reduce the effects of turbulence. For single-mode fibers, the use of adaptive optics can substantially improve the propagation efficiency. However, for multi-mode fibers, adaptive optics will have little effect on the propagation efficiency because the main contribution to the spreading angle is from diffraction due to poor beam quality, i.e., high value of M^2 .

To determine the merits of incoherently combining single-mode or multi-mode fiber lasers for DE applications, it is useful to compare their propagation efficiencies. Here, we define propagation efficiency as the ratio of power on target to total transmitted laser power. In making this comparison, the fiber laser systems are assumed to have the same size beam director and the same total power. Table 1 lists the parameters of four systems that are designed to deliver a total power of 100 kW. The systems are based on currently available fiber lasers. For example, for the 3 kW per fiber and $M^2 = 1$ case, 33 fiber lasers (N_{fiber}) are required to achieve 100 kW. The corresponding M^2 values reflect the fact

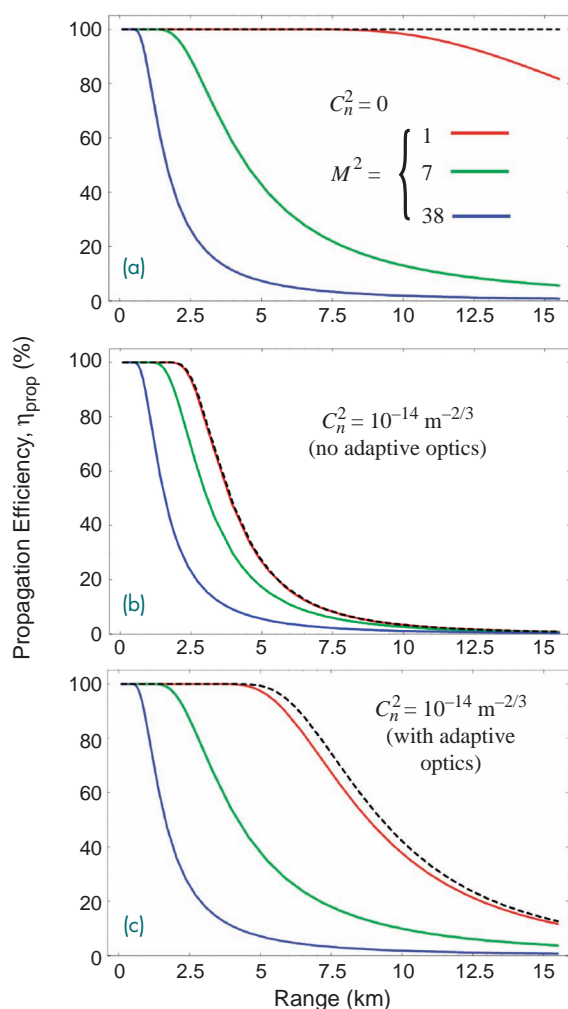
TABLE 1 — Four configurations of a 100 kW system using single-mode and multi-mode fiber lasers. Systems are labeled by color to match propagation efficiency plotted in Fig. 4. The black, dashed curve in Fig. 4 denotes an ideal Gaussian beam having a 50 cm spot size.

	Power/fiber (kW)	M^2	N_{fiber}	R_o (cm)
Red	3	1	33	8.7
Green	5	7	20	11.2
Blue	20	38	5	22.4
Black	100	1	1	50

that for multi-mode lasers the beam quality decreases (M^2 increases) as the power per fiber increases. Table 1 also gives the radius of the collimating lens for the individual fiber lasers (R_o). In all cases, the radius of the beam director is 50 cm and the target is assumed to be a circular disc with a surface area of 100 cm^2 . Figure 4 plots the propagation efficiency for $M^2 = 1, 7$, and 38 , in vacuum (Fig. 4(a)), and in a turbulent environment with $C_n^2 = 10^{-14} \text{ m}^{-2/3}$ (Figs. 4(b) and (c)). In all cases, the beams are focused onto the target. For propagation through turbulence, Fig. 4 shows the efficiency without adaptive optics (b) and with adaptive optics (c). The adaptive optics was modeled, in the results shown in Fig. 4(c), by increasing the Fried parameter by a factor of four. The dashed curves denote the case of a single ideal Gaussian beam with initial spot size equal to the radius of the beam director, i.e., the theoretical upper limit for perfectly coherently combined beams. For ranges $< 10 \text{ km}$ in vacuum (Fig. 4(a)), and for conditions in which turbulence dominates (Fig. 4(b)), the single-mode incoherently combined example (red curve) has a propagation efficiency virtually identical to that of the coherently combined beam (dashed curve), while the propagation efficiency of the various multi-mode fibers is far less. Figure 4 also shows that the use of adaptive optics can greatly improve the propagation efficiency of combined single-mode fibers but has little effect on the combined multi-mode fiber lasers.

Comparison of Incoherent and Coherent Combining

It is often stated that the advantage of coherent beam combining is that, for a given size beam director and total power level, coherent combining results in a smaller beam spreading angle compared with incoherently combined beams. For propagation in vacuum, the brightness (intensity/solid angle) of the coherently combined fiber array is N times larger than for an incoherently combined array, where N is the number


FIGURE 4

Propagation efficiency versus range for incoherently combined fiber laser beams with beam quality parameters $M^2 = 1, 7$, and 38 : (a) in vacuum, (b) in a turbulent atmosphere with $C_n^2 = 10^{-14} \text{ m}^{-2/3}$ (no adaptive optics), and (c) in a turbulent atmosphere with adaptive optics. Laser parameters are listed in Table 1. The dashed curve represents the theoretical upper limit for coherent and incoherent combining.

of fibers. While this is true for vacuum propagation, it is not relevant when the effects of atmospheric turbulence are taken into account. Beam brightness at the source is of limited importance when considering realistic DE propagation scenarios in turbulent atmospheres.

When the turbulence strength is large enough so that the Fried parameter, r_o , is less than the beam director radius, R_{BD} , coherent and incoherent combining give comparable values for spreading angle and spot size on target. This condition is usually satisfied for DE applications. For example, in moderate turbulence and a propagation distance of $L = 2 \text{ km}$, the Fried parameter is $r_o = 3 \text{ cm}$, which is typically much smaller than the beam director radius. As shown in Fig. 4(b), the power on target for an incoherently combined array of single-mode lasers with $N = 33$ (red curve) is virtually identical to that of a coherently combined array (dashed curve).

Compared to a coherently combined array, incoherently combined fiber lasers can deliver similar power levels to a remote target. This is seen by comparing the dashed (coherent array) and red (incoherent array)

curves in Fig. 4(a). For typical propagation scenarios and realistic atmospheric conditions, there is little if any advantage to coherently combining laser beams as compared to incoherently combining them.

Beam Wander and Tip-Tilt Compensation

Introducing tip-tilt correction into the individual steering mirrors can reduce the overall laser spot size on target. Tip-tilt correction redirects the centroids of the individual laser beams to cancel the effects of wander due to turbulence. This is accomplished by monitoring the intensity on target and redirecting the steering mirrors to minimize the spot size. Laser beam wander is a function of the scale size of the turbulence fluctuations. Turbulent eddies that are large compared to the laser beam diameter cause the laser beam centroid to be deflected and to wander in time due to transverse air flow. Eddies that are much smaller than the beam diameter cause spreading about the beam centroid and cannot be reduced by the use of tip-tilt compensation. The observed long time averaged laser spot size is a combination of beam wander and spread-

ing about the centroid. In weak turbulence, the beam centroid wander represents a significant contribution to the laser beam radius. As the turbulence level increases, or for long propagation ranges, the beam wander contribution to the laser spot size becomes less important. In very strong turbulence, the laser beam breaks up into multiple beams making tip-tilt compensation ineffective.

If the individual laser beams are separated by less than r_0 at the source, the wander of the centroids on the target will be correlated. In this case, it would be possible for beams to share a common tip-tilt correcting aperture, thus reducing the size and complexity of the system.

NRL FIBER LASER EXPERIMENTS

The NRL incoherent combining field propagation experiments use four IPG single-mode fiber lasers having a total output power of 6.2 kW (1 kW, 1.6 kW, 1.6 kW, and 2 kW). These initial experiments were performed at the Naval Surface Warfare Center (NSWC) in Dahlgren, VA, over a propagation range of 1.2 km. An aerial view of the propagation range is shown in Fig. 5. The laser beams propagated 4 to 10 ft above a blacktop road.

The beam director consists of four fiber output couplers and individually controlled steering mirrors which direct the four single-mode fiber laser beams onto a target. Each beam has a spot size of ~ 2.5 cm as it exits the beam director and the target is a 10-cm-radius, water-cooled power meter.

Figure 6 shows a schematic of the fiber laser output coupler and the beam expander (concave-convex lens combination) which is used to adjust the focal length. In these initial experiments the fiber lasers were operated at nearly half power because of thermal blooming in the beam director and in the atmosphere just beyond the laser source. These issues can be readily corrected in the next series of experiments by using lower-absorption optics and inducing air flow near the laser output. Thermal effects caused an axial shift of the focus with time as the total laser power was increased to ~ 3 kW. The change in the focal length was compensated for by changing the separation between the lenses in the beam expander. Figure 7 shows the beam director, output couplers, and steering mirrors used in the experiments.

The power on target as a function of time is shown in Fig. 8. After the output coupler reached thermal equilibrium (> 200 sec), the measured power was 2.8 kW, corresponding to a propagation efficiency of $\sim 90\%$. The typical errors associated with the measured transmitted power and power on target was $\pm 5\%$.

Atmospheric turbulence causes the laser beams on target to wander and change shape. Since the laser beam separation is initially much greater than r_0 , the

individual beams are uncorrelated and their centroids randomly wander with respect to each other. At times, the four beams completely overlap forming a single spot, while at other times the four individual beams are separated by typically a few centimeters. The characteristic time scale associated with beam wander is ~ 20 msec. Since the mechanical jitter angle was measured to be less than $\sim 2 \mu\text{rad}$, the beam centroid wander is caused mainly by atmospheric turbulence.

Figure 9 displays two frames from a CCD camera, the first at ~ 180 sec and the second at ~ 300 sec, showing 2.8 kW of combined laser power on the power meter. The two frames were chosen to illustrate cases where the four beam centroids are fully overlapped and where they have maximum displacement from each other. Precise measurements of beam wander and spreading at the target are difficult and were not available for these preliminary experiments because of pixel saturation in the camera and a limited number of frame samples. However, one can estimate the beam wander and spot size from the CCD images. The lower panel of Fig. 9 indicates that the average centroid wander was ~ 4 cm and that the individual instantaneous laser spot size was ~ 2.5 cm. Hence, the long time average spot size is estimated to be $R \sim 4.7$ cm.

To compare the experimental observations with simulations and theory, the atmospheric turbulence level, C_n^2 , was measured using a scintillometer. The average value of C_n^2 during the experiments was $\sim 5 \times 10^{-14} \text{ m}^{-2/3}$ and the average transverse wind velocity was estimated to be ~ 2.5 m/sec.

Comparison of Experiments with Simulations and Theory

The Navy's High-Energy Laser Code for Atmospheric Propagation (HELAP)^{3,4,5} was used to model the propagation experiments. The HELAP code is



FIGURE 5
Aerial view of the laser propagation range in Dahlgren, VA.

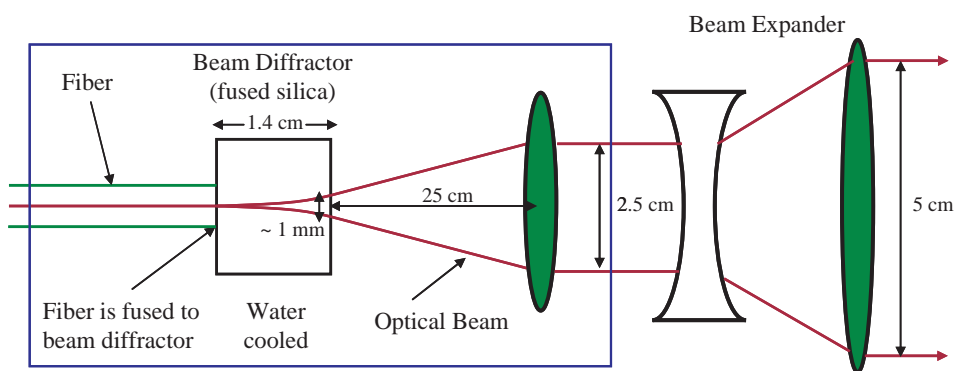


FIGURE 6
Schematic diagram of fiber output coupler and beam expander.

FIGURE 7
Beam director used for incoherent combining. Three of four fiber output couplers are shown in the foreground. Four individually controlled steering mirrors are shown in the background.

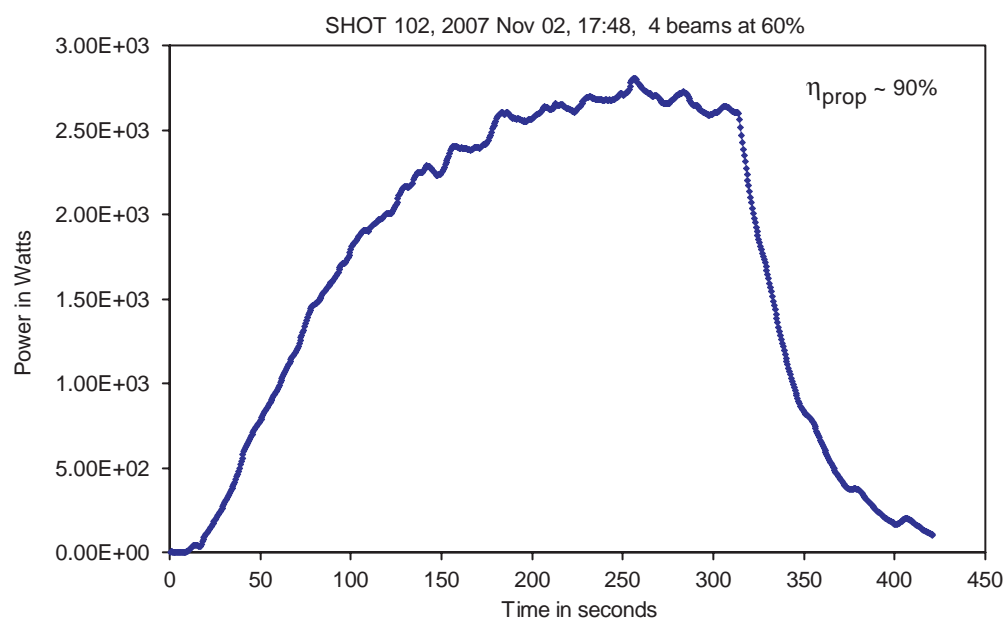
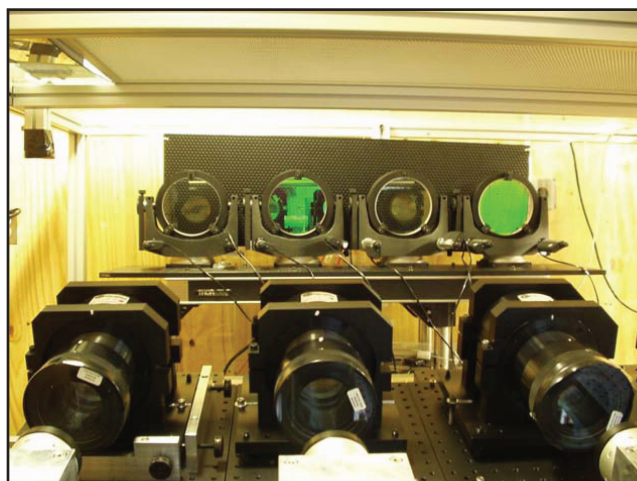
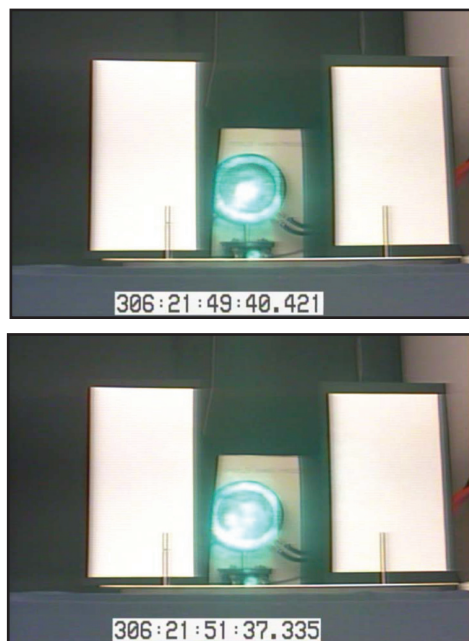


FIGURE 8
Experimentally measured power at target versus time. Target was a power meter with 45 sec response time and 10 cm radius. Average wind speed was ~ 2.5 m/sec, and measured turbulence strength $C_n^2 = 5 \times 10^{-14} \text{ m}^{-2/3}$. The maximum propagation efficiency is $\sim 90\%$. Thermal equilibrium in the power meter is reached at ~ 200 sec and the laser beams are turned off at ~ 320 sec.

**FIGURE 9**

Two CCD camera images of four beams incoherently combined on target (10 cm radius power meter) at a range of 1.2 km. The first panel shows the combined beams at ~180 sec and the second image is at ~300 sec. The later image shows the four individual beam centroids randomly displaced by ~4 cm due to atmospheric turbulence.

fully three-dimensional, time-dependent, and includes molecular/aerosol scattering/absorption, turbulence, and thermal blooming effects. The simulations assume an aerosol scattering coefficient of 0.05 km^{-1} and $1 \text{ } \mu\text{rad}$ of mechanical jitter.³

Figure 10 shows the results of HELCAP simulations in which four laser beams, with a total power of 3 kW and at a range of 1.2 km, were incoherently combined. Panel (a) shows the intensity contours of the four beams at the fiber laser output coupler. The focal length of each beam was adjusted to minimize the spot size on target. Panel (b) shows time-averaged (over a few seconds) intensity contours of the combined laser beam on the target plane. The long time average spot size on target from the simulations was ~4.6 cm compared with the experimental estimate of 4.7 cm. The intensity profile as a function of time indicates that the rms wander displacement from the simulations was ~2.5 cm compared with the experimental estimate of 4 cm. The instantaneous spot size of the individual beams from the simulations was ~3.1 cm compared with the experimental estimate of 2.7 cm.

Using atmospheric turbulence theory^{3,6,7} we calculated the laser beam wander displacement and long time averaged spot size. The calculated beam wander and long time average spot size was 2.8 cm and 4.2 cm, respectively. These calculated values are in good agreement with experimental observations and HELCAP simulations.

DISCUSSION

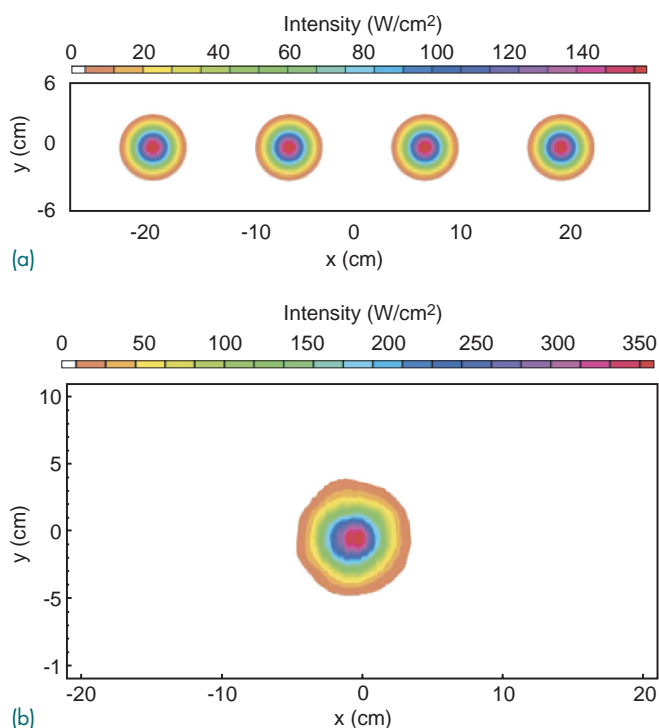
In 2008, the NRL fiber lasers will be moved to the Starfire Optical Range in Albuquerque, NM, and

propagation experiments over a 3.2 km range will take place at full power. The objectives of these experiments are to demonstrate the incoherent beam combining concept at longer range, quantify thermal blooming effects, more precisely characterize the beam wander and spreading, and validate the propagation model (HELCAP). Planned experiments will incorporate target-in-the-loop tip-tilt compensation into one of the fiber laser beams to correct for wandering of the beam centroid. Controlled thermal blooming experiments can also be carried out using a stagnation tube to eliminate the cooling effects of transverse air flow. This arrangement permits thermal blooming effects to be observed under controlled conditions and at relatively low power levels. The temporal change in the laser spot size and intensity and measurements of the air properties inside the stagnation tube will provide the necessary data to study atmospheric thermal blooming under realistic conditions.

In addition to the NRL program, other fiber laser-based DE efforts are underway. A NAVSEA lethality/propagation program being carried out at NSWC Dahlgren utilizes six multi-mode fiber lasers, each having a CW power of 5 kW and optical quality of $M^2 \sim 6$. A joint Pennsylvania State University/NSWC Crane lethality and propagation program is also under way using two multi-mode fiber lasers, 10 kW ($M^2 \sim 13$) and 5 kW ($M^2 \sim 6$).

SUMMARY

Incoherent combining of high-power fiber lasers can result in highly efficient, compact, robust, low-maintenance, and long-lifetime high-energy laser

**FIGURE 10**

HELCAP simulation showing a time-averaged transverse intensity profile of laser beams at (a) the source and (b) incoherently combined on target at a range of 1.2 km. The atmospheric turbulence level used in the simulation is the same as those measured in the experiment.

systems for directed-energy applications. In this article, we discussed the propagation of incoherently combined single-mode and multi-mode fiber laser beams through atmospheric turbulence. We compared the propagation efficiency of coherent and incoherent combining and found that under typical atmospheric conditions and propagation ranges, the propagation efficiency of incoherently combined single-mode fiber lasers is nearly identical to the theoretical upper limit for coherent combining. Hence, there is no inherent advantage to coherently combining beams for tactical directed-energy scenarios.

We presented results from the first field demonstration experiments of long-range incoherent combining. The experiments combined four fiber lasers using a beam director consisting of individually controlled steering mirrors. Propagation efficiencies of ~90%, at a range of 1.2 km, with transmitted CW power levels of 3 kW were demonstrated in moderate turbulence. Numerical simulations and theoretical results were in good agreement with experimental observation.

The NRL propagation experiments have provided important information concerning the issues associated with incoherently combining high-power, single-mode fiber lasers. These field experiments will lay the groundwork for developing a tactical DE laser system in the near term.

ACKNOWLEDGMENTS

We acknowledge C. Rollins, G. Dicomio, Z. Wilkes, and J. Caron for their assistance in the field experiments.

[Sponsored by NRL, ONR, and HEL-JTO]

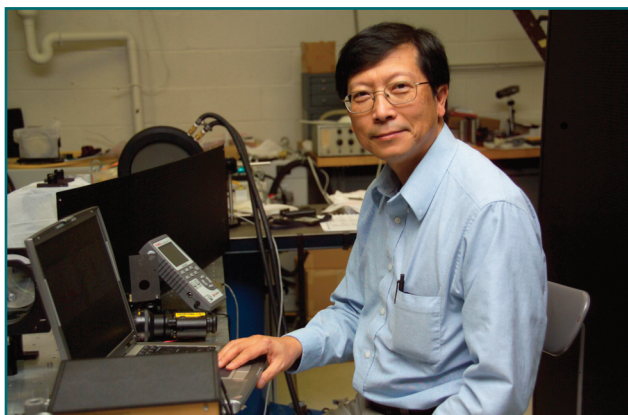
References

- ¹ V. Gapontsev et al., "2 kW CW Ytterbium Fiber Laser with Record Diffraction-Limited Brightness," in *2005 Conference on Lasers and Electro-Optics Europe (CLEO Europe)*, p. 508 (2005).
- ² J. Edgcombe, "Kilowatt Level, Monolithic Fiber Amplifiers for Beam Combining Applications at 1 μ m," *Proceedings of the 20th Solid State and Diode Laser Technology Review* (2007).
- ³ P. Sprangle, J. Peñano, B. Hafizi, and A. Ting, "Incoherent Combining of High-Power Fiber Lasers for Long-Range Directed Energy Applications," *Journal of Directed Energy* **2**, 273-284 (2007); also NRL Memorandum Report, NRL/MR/6790--06-8963, June 2006.
- ⁴ P. Sprangle, J. Peñano, and B. Hafizi, "Optimum Wavelength and Power for Efficient Laser Propagation in Various Atmospheric Environments," *Journal of Directed Energy* **2**, 71-95 (2006).
- ⁵ J.R. Peñano, P. Sprangle, and B. Hafizi, "Propagation of High Energy Laser Beams Through Atmospheric Stagnation Zones," *Journal of Directed Energy* **2**, 107 (2006).
- ⁶ L.C. Andrews and R.L. Phillips, *Laser Beam Propagation through Random Media*, 2nd ed. (SPIE Press, Bellingham, WA, 2005).
- ⁷ R.L. Fante, "Electromagnetic Beam Propagation in Turbulent Media," *Proc. IEEE* **63**, 1669-1692 (1975). ★

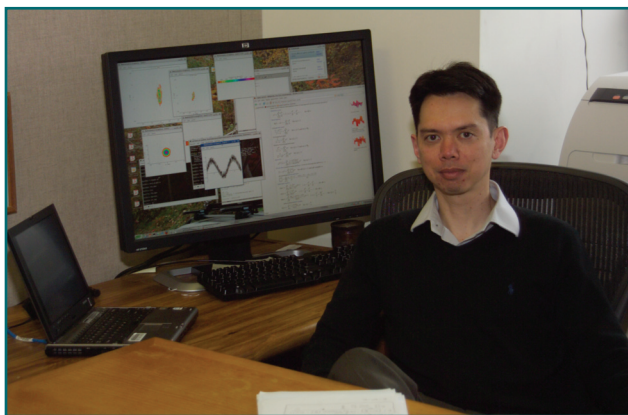
THE AUTHORS



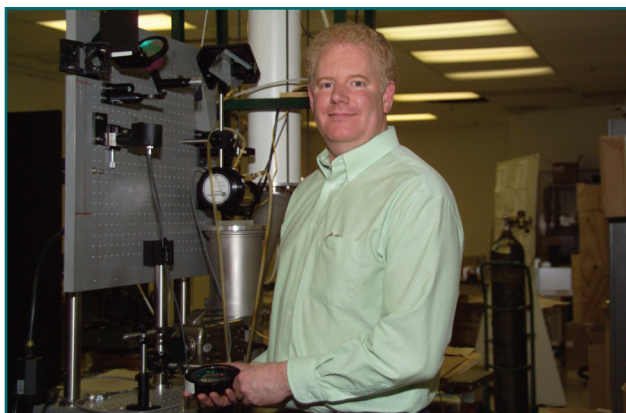
PHILLIP SPRANGLE is chief scientist and head of the Beam Physics Branch of the Plasma Physics Division at NRL. He received a Ph.D. in physics from Cornell University in 1973. Dr. Sprangle's primary areas of research include high-energy and high-intensity laser physics, free-electron lasers, nonlinear optics, and laser plasma accelerators. Dr. Sprangle is the recipient of the 1986 E. O. Hulburt Science Award, the 1991 International Free Electron Laser Prize, the 1994 Sigma Xi Pure Science Award, and the IEEE Plasma Science and Applications Award. Dr. Sprangle is a Fellow of the American Physical Society, IEEE, and the Directed Energy Professional Society, and a member of Sigma Xi.



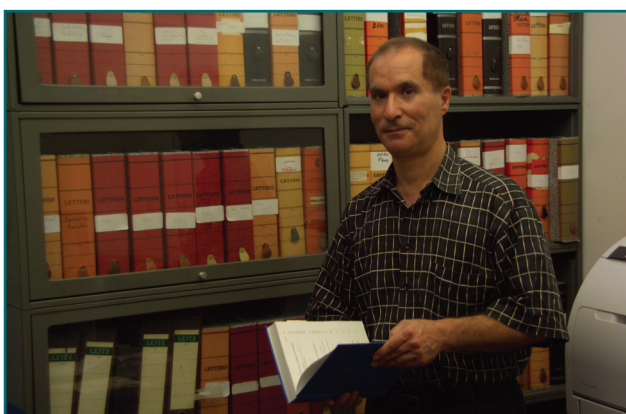
ANTONIO TING is head of the Laser Physics Section and a senior research physicist in the Beam Physics Branch of the Plasma Physics Division at NRL, where he has worked since 1988. His research areas include ultra-high-field physics, advanced particle accelerators, advanced radiation sources, and intense laser interactions with air, plasmas, and electron beams. Dr. Ting has published 101 refereed journal articles and holds three U.S. patents. He has presented 23 invited and review talks at professional and international conferences. He is a Fellow of the American Physical Society and member of Sigma Xi. He has twice won the NRL Alan Berman Publication Award and the 2003 *NRL Review* Award.



JOSEPH PEÑANO is head of the Radiation and Acceleration Physics Section of the Plasma Physics Division at NRL. He received a Ph.D. in physics from the University of California, Los Angeles, in 1998 and joined the NRL Plasma Physics Division in 2002. His research areas include high-energy and high-intensity laser physics; atmospheric propagation of high-energy and ultra-short-pulse lasers, interactions of intense ultra-short lasers with dielectric materials, detection of special nuclear materials, free-electron lasers, and laser plasma accelerators. Dr. Peñano holds two U.S. patents and is a winner of the 2002 NRL Alan Berman Publication Award, the 2003 Directed Energy Professional Society Best Paper Award, the *NRL Review* Featured Research Award in 2003, 2004, and 2008, and the 2003 NRL Technology Transfer Award.



RICHARD FISCHER received his B.S., M.S., and Ph.D. degrees in electrical engineering from the University of Maryland, College Park, in 1984, 1986, and 1993, respectively. He has been a researcher in the Plasma Physics Division at NRL since 1988. His recent research has concentrated on atmospheric laser propagation and the interaction of intense lasers with electron beams, semiconductors, and plasmas. This includes experiments on high-power fiber laser propagation, relativistic Thomson backscattering, athermal annealing of semiconductors, and the development of gyrotrons, quasioptical gyrotrons, and quasioptical gyroklystrons. Dr. Fischer is a member of the American Physical Society.



BAHMAN HAFIZI received B.Sc. and Ph.D. degrees in physics from Imperial College, London, in 1974 and 1978. He is president of Icarus Research, Inc., and a theoretical research scientist at NRL. He previously worked as a research associate in the Department of Astro-Geophysics at the University of Colorado and as a staff scientist for Science Applications International Corporation. His current research areas include propagation of ultra-intense laser pulses, laser-driven electron accelerators, free-electron lasers, laser-plasma interactions, and nonlinear optics. He has also worked on advanced sources of electromagnetic radiation and ultra-broadband sources, with application to imaging, lithography, and remote sensing. He is an Associate of the Royal College of Science and a member of the American Physical Society, the European Physical Society, and the IEEE.